Order-disorder character of the hydrogen bond in KH_2PO_4

Paulo R. P. Silva and J. A. Roversi*
Instituto de Fisica "Gleb Wataghin," Universidade Estadual de Campinas, C.P. 1170 - Campinas, SP., Brasil
(Received 30 August 1979)

A discussion is presented on some of the available evidence for the shape of the local effective potential for the hydrogen motion in KDP-type ferroelectrics, particularly regarding the existence or nonexistence of a central barrier in that potential. For this purpose a one-minimum square-well potential model is considered and compared with the corresponding tunneling model. The comparison of results so obtained for both models with available experimental data on the isotope dependence of the critical temperature, Curie constant, and maximum spontaneous polarization at absolute zero leads to the conclusion that the accuracy of the experimental data together with the uncertainties on the theoretical calculations do not yet permit a discrimination in favor of an order-disorder double-well character for these ferroelectric crystals.

I. INTRODUCTION

The most outstanding feature of the KH_2PO_4-type ferroelectrics is the strong dependence of their electric and thermal properties on the replacement of the protons by deuterium, namely the isotope effect.[1-5]

The crystals of the KDP family are all uniaxial tetragonal in the paraelectric phase. In the polarized state the spontaneous electric polarization occurs along the c axis, whereas the Bacon and Pease[6] (BP) neutron-diffraction experiments have shown that the hydrogen motion is almost completely restricted to the a-b plane[7] along the O—H—O bond. Apparently, this is a curious result in view of the strong isotope effect known to exist in these materials. In the case of KDP, the assumption of valence K^{1+} and P^{3-} ions, in addition to the use of observed equilibrium displacements of these ions along the c axis led Bacon and Pease to an estimate of the saturation polarization close to the observed value. According to Jona and Shirane[2] (JS), the charge assignment suggested in BP produces the wrong sign for the electric polarization if use is made of the observed K and P displacements. For this reason they proposed instead the assignment K^{1+}, P^{5+}, and O^{2-}, obtaining for the maximum spontaneous polarization, P_M, at absolute zero temperature, a magnitude still consistent with experiments but with sign opposite to that obtained by BP. As quoted by JS the configuration of KDP displacements has been determined by means of the anomalous dispersion of x rays by Unterleitner *et al.*[8] with the result that the JS assignment is the one that is consistent with experiments. In any event a clarification of the appropriate charge assignment and the corresponding ionic displacements from para- to ferrophase would be of importance in the theory for the O—H—O bond in KDP. An independent check on the ionic charge state of K,P as well as O ions by other methods such as ultraviolet spectroscopy, electron paramagnetic resonance (EPR), or nuclear quadrupole resonance (NQR) does not seem to be available yet.

The strong deuteration dependence of the electric and thermal properties makes it necessary to include in the theory a coupling between the heavy-ion coordinates and those of the hydrogens. If we recall that the hydrogen mass m appears in the *ab initio* Hamiltonian in the form $(\hbar^2/2m)(d/du)^2$ it becomes clear that the isotope effect is equivalent to the quantum effect; in other words, the neglect of quantization prevents one from describing the isotope effect. For this reason it is convenient to call the KDP-type ferroelectrics quantum ferroelectrics.

Another ingredient customarily employed in microscopic-model Hamiltonians for these ferroelectric crystals is the inclusion of a one-particle local symmetric potential $V_s(u)$ for the anharmonic motion of the hydrogen atom along the O—H—O bond. The form of the local potential $V_s(u)$ has been considered of such a paramount importance in the literature that its shape has been taken to provide a criterion for a classification of ferroelectric crystals in two groups: displacive ferroelectrics and order-disorder ferroelectrics; the former types requiring a nearly harmonic one-minimum potential, and the latter group requiring a central-barrier double-well (DW) symmetric potential.

It is the purpose of the present paper to discuss some of the available evidence on the shape of the symmetric local potential, $V_s(u)$, in particular regarding the existence or nonexistence of a central barrier for the hydrogen motion along the O—H—O bond in KDP. With this objective in mind, the most simple one-minimum anharmonic potential, i.e., Pirenne square-well (SW) potential,[9] is considered. In Secs. III and IV the isotope dependence of the critical temperature T_c, the Curie constant near the critical point C_c, and P_M is obtained. In Sec. V the corresponding

results for the double-well tunneling model[10–13] are listed. The comparison of both models with the experimental results is presented in Sec. VI.

In order to fix our ideas, it seems convenient to specify the assumptions of the microscopic model Hamiltonian, which may be considered to be the following: (i) The anharmonic hydrogen motion along the O–H–O bond occurs only in the a-b plane, even with the application of an electric field along the c axis. Along these lines, the hydrogen coordinates transverse to the bond are also ignored, or in other words the assumption is made that the hydrogens do not interact directly with the applied field and do not contribute directly to the electric polarization. (ii) In order to reduce the number of adjustable parameters of the problem, the hydrogen mass should appear explicitly by means of the hydrogen kinetic energy $(\hbar^2/2m)(d/du)^2$. In other words, an adequate description of the isotope effect appears here as directly connected with the appropriate account of quantization. (iii) A strong short-range correlation is assumed to exist among the four nearest-neighbor hydrogen atoms leading to a reduction in the number of hydrogen coordinates to one for each KH_2PO_4 molecule. (iv) In the limit of strong short-range interaction between the KP-dipole coordinate and its associated hydrogen atom, the heavy-ion coordinates may be ignored if use is made of a relation of type

$$P_z(j) = Z^* e u_j \ , \tag{1.1}$$

where $P_z(j)$ is the c-axis electric dipole of KP ions in molecule j, Z^*e is a constant with dimension of an electric charge, and u_j is the hydrogen coordinate along the bond measured from its center. (v) The hydrogen atoms interact among themselves through mediation of the direct, long-range, dipole-dipole interaction existing between the KP electric dipoles, resulting in a bilinear Ising-type coupling of the form $-\sum_i \sum_{j\neq i} J_{ij} u_i u_j$ (see Appendix).

The model Hamiltonian in the presence of an uniform electric field $\vec{E} = E\hat{z}$ along the c axis of the crystal is taken as

$$H = \sum_j \left(\frac{p_j^2}{2m} + V_s(u_j) \right) - \tfrac{1}{2} \sum_i \sum_{j\neq i} J_{ij} u_i u_j - Z^* e E \sum_j u_j \ , \tag{1.2}$$

where the last term results from Eq. (1.1), and the quantity E should be interpreted as the internal field. The indices i and j refer to KDP molecule sites, that is, $j = \vec{R}_j$, and the dimensionality of the lattice is specified by the dimensionality of vector $\vec{R}_j$; the displacement operator u_j is actually an infinite matrix with eigenvalues in the range $(-\frac{1}{2}a) \leq u_j \leq (\frac{1}{2}a)$. A similar Hamiltonian has been considered by Lines.[14]

In the above equation $V_s(u)$ is the so-called one-particle local anharmonic symmetric potential for the hydrogen motion along the O–H–O bond; $V_s(u)$ will be the center of our discussion. The form of $V_s(u)$ as well as its one-body or many-body character have been a much-studied and -debated subject in the last 40 years.[15–17] It is shown in the present paper that, as far as the quantum ferrolectrics are concerned, the form and the nature of the hydrogen motion in the O–H–O bond are unsettled matters open to discussion even to date. Moreover it is necessary to note that the O–H–O bonds of KDP-type ferroelectrics are in the intermediate critical region between short and long hydrogen bonds, i.e., very close to the maximum in Fig. (2.7) of Hamilton's book.[17] According to Huggins,[18] the form of the "local" hydrogen potential in O–H–O bonds is sensitive to the O–O distance as well as to any possible charge fluctuations of the oxygen ions. Here we note that the d(O–O) dependence may become particularly strong near the sharp maximum of the curve for the O_1H covalent bond length versus O–O distance.

A sizable charge fluctuation of the oxygen ions was observed by Blinc[19] in a NQR experiment on ^{75}As, and that charge fluctuation was associated with the hydrogen motion in KH_2AsO_4.

In summary it may be stated that the O–O zero-point stretching vibrations considered by Reid,[20] in addition to the problem of oxygen charge fluctuations[19] and ionic polarizabilities,[1] will probably lead to a many-body character for the "local" effective one-particle potential for the hydrogen motion, or in other words, $V_s(u)$ may become temperature dependent, as in the work of Mason[20] for Rochelle salt.

Even if the idea of an "effective" one-particle potential is accepted for KDP-type ferroelectrics, the expansion of the O–O distance observed by Ubbelohde *et al.*[21] in KDP, when the protons are replaced by deuterons, seems to indicate that the form of the effective $V_s(u)$ for O–D–O may be different from that of the local potential for O–H–O. Even so, this possibility will not be considered in the present paper. It is convenient to recall that here one is concerned with small quantities such as the presence or absence of a central barrier in the effective local potential.

In view of the above discussion, it seems clear that the choice of the form of $V_s(u)$ as establishing a criterion for a classification of ferroelectric crystals has been a particularly unfortunate one, at least for the quantum ferroelectrics, where the use of a one-particle potential seems to be already an oversimplification.

In spite of that, in the framework of the above oversimplification, in the present paper, we consider

the simplest possible potential without a central barrier, which is Pirenne square-well (SW) potential.[9]

We believe that the Hamiltonian Eq. (1.2) in its own right deserves a careful examination, and an exact solution would be highly desirable. An exact quantum-mechanical treatment of the above Hamiltonian, for two- and three-dimensional lattices seems to be a formidable task at the moment. The analogous Heisenberg and Ising quantum-spin Hamiltonians have been studied thoroughly in the last 50 years. In 1944 Onsager[22] succeeded in obtaining an exact solution for the Ising half-spin case, with nearest-neighbor interactions, concluding that two-dimensional lattices do have a ferromagnetic phase transition. As for the quantum Heisenberg (QH) Hamiltonian with isotropic nearest-neighbor interactions for three-dimensional lattices, only recently (1976) has an exact proof been found by Dyson, Lieb, and Simon.[23] They showed in their important work the existence of a ferromagnetic ordering at temperatures below a certain $T^*(\leq T_c)$; in view of that work, it seems unbelievable that the quantum Hamiltonian Eq. (1.2) does not produce a ferroelectric phase transition.

It should be noted that during these 50 years, the Heisenberg Hamiltonian has been used[24] to improve our understanding of the ferromagnetic materials even in the absence of an exact proof for the existence or nonexistence of a magnetic phase transition. It should also be mentioned that most of these achievements would have been impossible without the use of the Weiss molecular-field approximation (MFA).

As far as the calculation of the critical temperature T_c is concerned, there are strong indications based on the Onsager reaction field approximation[25] (ORFA) that the MFA, for the QH-nearest-neighbor Hamiltonian in simple-cubic lattices is in error by being about 30% higher than the correct value.

No similar calculations for T_c in the case of the pure, long-range, quantum dipole-dipole interaction spin Hamiltonian, in three-dimensional lattices, are known to the present authors. It is quite possible that in this case, for a long-range interaction, both MFA and ORFA approximations should produce about the same result for T_c, at least within a relative error smaller than 30%.

On the other hand, as shown in Sec. V, the experimental data for parallel electric susceptibility of KDP are well described by the present model in the MFA, even in the region $|T-T_c| \ll T_c$, where the effects of renormalization-group theory[26] are expected to become important. In our opinion the reason for the success of the MFA in KDP resides in that it allows for the exact consideration of the quantum and the full anharmonic character of the problem, allied to the actual long-range feature of the dipole-dipole interaction, which seems to play an important role in KDP. The application of the square-well potential to KDP and DKDP is presented in Sec. VI, where, as a result of the calculations, the values of J_{ij} required to reproduce the experimental values of $T_c(H)$ and $T_c(D)$ turn out to be roughly of the order of magnitude of the dipole-dipole interaction, i.e.,

$$J_{ij}a^2 \simeq p_s^2/r_{ij}^3 \ , \tag{1.3}$$

where p_s is defined in Eq. (1.16).

In view of the above discussion, if in Eq. (1.2) we replace u_j by the expression

$$u_j = \langle u_j \rangle + x_j \ , \tag{1.4}$$

where $\langle u_j \rangle = \bar{u}$ is the thermal average of u_j and x_j is the fluctuation, one obtains

$$H = \sum_j H_L(u_j) - \tfrac{1}{2} \sum_i \sum_{j \neq i} J_{ij} x_i x_j + \tfrac{1}{2} N J \bar{u}^2 \ ; \tag{1.5}$$

the MFA corresponds to keeping only the first (separable) term in Eq. (1.5) and neglecting bilinear terms in the fluctuations. The local effective "polarized" Hamiltonian $H_L(u)$ is given by

$$H_L(u) = H_0 + H_p \ , \tag{1.6}$$

$$H_0(u) = p^2/2m + V_s(u) \ , \tag{1.7}$$

where $V_s(u)$ is the infinite square-well potential of width a, and H_p, the polarization contribution, is given by

$$H_p = -Au \ , \tag{1.8}$$

$$A = J\langle u \rangle + Z^* eE \ , \tag{1.9}$$

$$J = \sum_{l \neq 0} J_{0l} \ ; \tag{1.10}$$

J is assumed to be positive. In the Appendix an heuristic argument is presented to justify this assumption. The total partition function Z of the system in the MFA factors as

$$Z = (Z_L)^N , \tag{1.11}$$

where we have dropped a constant factor, and N is the total number of dipoles, i.e., the total number of KH_2PO_4 molecules,

$$Z_L = \mathrm{Tr}(e^{-\beta H_L}) \tag{1.12}$$

is the local partition function, and

$$\langle u \rangle = \mathrm{Tr}(u e^{-\beta H_L})/Z_L \ , \tag{1.13}$$

where H_L is defined in Eq. (1.6).

We also note that the above model contains only two independent energy parameters, E_c and W, where

$$E_c = \pi^2 \hbar^2 / 2ma^2 \tag{1.14}$$

is related to H_0, and

$$W = Ja^2 \ ; \tag{1.15}$$

the third parameter, with the dimension of a dipole moment is

$$p_s = \tfrac{1}{2} Z^* ea \ , \tag{1.16}$$

where Z^*, defined in Eq. (1.1), establishes the connection between the dynamics of the hydrogen motion and the polarization properties of the system.

If we compare the number of independent parameters of the present no-barrier model with that of the pseudospin Hamiltonian,[11] we have to recall that

$$H_{ps} = 2\Omega_T \sum_j X_j - \tfrac{1}{2} \sum_i \sum_{j \neq i} F_{ij} Z_i Z_j \ , \tag{1.17}$$

where X_j, Y_j, and Z_j are the corresponding dimensionless 2×2 pseudospin Pauli matrices for the hydrogen atom j, Ω_T is the tunneling energy, and F_{ij} is a hydrogen-hydrogen coupling. In the MFA both models present three independent parameters, which are E_c, W, and p_s, in the no-barrier model [see Eqs. (1.14)–(1.16)]. In the pseudospin model, the corresponding parameters are Ω_T, F, and μ, where $F = \sum_j F_{0j}$.

In the pseudospin model it is customary to assume $F(\mathrm{H}) = F(\mathrm{D})$ and $\mu(\mathrm{H}) = \mu(\mathrm{D})$, where H and D means KH_2PO_4 and KD_2PO_4, respectively; Ω_T is to be adjusted independently for the protonic and the deuterated cases, whereas, in the no-barrier model discussed in this paper, it is assumed that $W(\mathrm{H}) = W(\mathrm{D})$, $p_s(\mathrm{H}) = p_s(\mathrm{D})$, and once $E_c(\mathrm{H})$ is specified, $E_c(\mathrm{D})$ is taken as $E_c(\mathrm{D}) = \frac{1}{2} E_c(\mathrm{H})$, as one obtains from Eq. (1.15), assuming $a(\mathrm{H}) = a(\mathrm{D})$.

It is also important to observe that most of these theories when checked and adjusted to some particular experimental data give rise to parameter values which make impossible the quantitative description of the remaining available experimental information. All of them seem to be qualitatively adequate to describe the thermal, electric, or optical properties of the quantum-ferroelectric crystals, sometimes with numerical relative errors of a few to 50 percent.

In other words, it is the opinion of the present authors at this stage that the precision of the available theories, i.e., the theoretical errors introduced by the various required approximations, as well as the precision of the available experimental data, are not yet adequate for a specification of the details of the local potential, such as the existence or nonexistence of the central barrier in KDP-type ferroelectrics.

One should also note that, if we call KH_2PO_4 and KD_2PO_4 an associated pair, it follows that, for each *associated pair* of quantum ferroelectrics, the present no-barrier model contains only three independent parameters, whereas the pseudospin model of Eq. (1.17) presents four independent adjustable parameters.

The ratio of the two energies E_c and W in Eqs. (1.14) and (1.15) defines a dimensionless parameter

$$\gamma = E_c / W \ , \tag{1.18}$$

which represents a measure of the relative importance of the quantum effect in the problem. The classical limit corresponds to $\gamma \to 0$.

As a preliminary study of the local partition function Z_L in Eq. (1.12), in Sec. II its classical statistical mechanical (CSM) treatment is presented, with the result that the Hamiltonian Eq.(1.6) reproduces the Weiss MFA as applied to the Langevin theory of classical dipoles,[27] and with the conclusion that, in the limit $\gamma \to 0$, a second-order ferroelectric phase transition is obtained with

$$kT_c(cl) = \tfrac{1}{12} W \ , \tag{1.19}$$

where W is defined in Eq. (1.15).

In Sec. III the exact quantum-statistical mechanical (QSM) calculation of Z_L is considered, having in mind the limited purpose of finding the solution of the self-consistent conditions for $\bar{u}$, as well as determining carefully the order of the possible transition. It turns out that a second-order phase transition is obtained; defining

$$\tau_c = T_c / T_0 \ , \tag{1.20}$$

where T_0 is defined in Eq. (2.9), a curve is obtained in Fig. 3 for τ_c as a function of the dimensionless quantum parameter

$$\gamma^* = \gamma / \gamma_s \ , \tag{1.21}$$

where γ is defined in Eq. (1.18) and γ_s, in Eq. (3.13).

The static, uniform electric parallel susceptibility along the c axis in the paraphase is also considered in Sec. III for arbitrary temperatures above T_c. The fact that the experimental behavior of the susceptibility follows quite closely the Curie law near the critical point is a result that probably is related to the long-range character of the dipole-dipole interaction. The Curie constant C_c, close to the critical point, as obtained in Eq. (3.17), has a value quite different from C_f, the Curie constant in the high-temperature limit, where the dipoles are classical and nearly free. In the region $T >> T_0 = T_c(cl)$, the susceptibility should be replaced by the classical expression

$$\chi = C_f / (T - T_0) \ , \tag{1.22}$$

where

$$C_f = N p_s^2 / 3k \ , \tag{1.23}$$

N is the total number of dipoles (i.e., the total number of KDP molecules); p_s is defined in Eq.

(1.16), k is the Boltzmann constant, and T_0 is the paraelectric[28] temperature which should be obtained by the usual straight-line extrapolation of $1/\chi$ from the high-temperature region. The fact that C_c is different from C_f is another manifestation of the importance of the quantum effect. In Fig. 4 a curve is displayed for C_c/C_f versus γ^*.

It is also necessary to point out that precaution has to be taken in extrapolating the high-temperature (classical) expression for the susceptibility to temperatures close to T_c, where the quantum effects are important. We also believe that a clarification of the appropriate extrapolation procedure $T \rightarrow T_c$ will be of interest in the discussion concerning the so-called soft model[13,29] in quantum ferroelectric crystals. Also note that, as a result of the application of the present model to the associated KDP and DKDP pair, it turns out that in KDP T_c is less than T_0, and this result seems to favor the imaginary coupling considered by Scarparo *et al.*[29]

In the SW model considered here, it is impossible to obtain the temperature dependence of the spontaneous polarization $P(T)$ in the whole ferroelectric phase in terms of closed expressions. Even the point-by-point self-consistent computer calculation is complicated by the requirement of certain Airy functions. For this reason, in the present paper, Sec. IV, the discussion of the spontaneous polarization will be limited to the γ^* dependence of the maximum polarization P_M at $T=0$ K.

Section V is a brief description of the Tokunaga and Matsubara[12] (TM) tunneling pseudospin model in the framework of MFA, where we have singled out the classical limit to simplify the discussion. In that model they obtained a second-order phase transition for arbitrary values of the quantum parameter q in the range $0 < q < 1$; this quantum parameter is the analog to γ^* in the square-well model. Curves for the isotope dependence of T_c, C_c, and P_M in that model are given in Sec. V.

Both models lead to a second-order ferroelectric phase transition, if use is made of the MFA. The cluster approximation applied by TM to the tunneling model also gives rise to a second-order phase transition for finite arbitrary values of their parameter n; a first-order transition only occurs in the Slater[30] limit $n \rightarrow \infty$. The first experimental evidence to the effect that in KDP the transition could be of first-order type, came from work by De Quervain.[31] The beautiful x-rays-dilatometric studies in KDP by Kobayashi *et al.*[32] led these workers to the conclusion that the transition is unequivocally one of first order. Dielectric,[33] calorimetric,[34] and electrocaloric[35] studies, as well as the electric-field dependence of the polarization[36] in a region around the ferroelectric transition of KDP also provide clear evidence in favor of a first-order phase transition.

Among the papers suggesting theoretical models[37] able to display a first-order transition for KDP-type ferroelectrics, no detailed discussion seems to have been presented on the quantitative aspects of the deuteration dependence of T_c, C_c, and P_M. The long-overdue necessity for a quantitative comparison between the consequences of the square-well model and the corresponding ones for the tunneling TM model, seems to warrant an application of the results presented in Secs. III, IV, and V for the isotope dependence of T_c, C_c, and P_M to the associated (KH_2PO_4, KD_2PO_4) pair. Such a comparison is presented in Sec. VI.

In Sec. VII a brief discussion is presented on the interpretation of hydrogen-associated infrared and Raman frequencies in terms of the one-minimum or double-well character of the "local" potential.

II. CLASSICAL APPROXIMATION

In the framework of the MFA described above, and in the classical limit, the local partition function Z_L, up to a constant factor, may be written

$$Z_L = \int_{-\infty}^{+\infty} \exp(-\beta p^2/2m)\, dp \times \int_{-\infty}^{+\infty} \exp\{-\beta[V_s(u) - Au]\}\, du \quad , \tag{2.1}$$

$$Z_L = \int_{-a/2}^{+a/2} \exp(\beta A u)\, du \quad , \tag{2.2}$$

where we have dropped the factor from the kinetic-energy part. The thermal average of u_j,

$$\langle u \rangle = \frac{1}{\beta} \frac{\partial \ln Z_L}{\partial A} \quad , \tag{2.3}$$

is given by

$$\frac{\langle u \rangle}{\frac{1}{2}a} = \frac{1}{\tanh\xi} - \frac{1}{\xi} \quad , \tag{2.4}$$

$$\xi = \tfrac{1}{2}\beta A a \quad , \tag{2.5}$$

where A still depends on $\langle u \rangle$, as explained in Eq. (1.9). The self-consistency condition corresponds to finding the common root of $F(\xi) = G(\xi)$, where $F(\xi) = L(\xi)$ is the Langevin function for classical dipoles

$$F(\xi) = \frac{1}{\tanh\xi} - \frac{1}{\xi} \quad , \tag{2.6}$$

$$G(\xi) = \frac{4kT}{W}(\xi - \xi_0) \quad , \tag{2.7}$$

where F comes from Eq. (2.4) and G comes from Eq. (1.9), with

$$\xi_0 = p_s E/kT \quad . \tag{2.8}$$

The self-consistent root ξ_{sc} also determines the self-consistent value of the polarization, $\langle u\rangle/\frac{1}{2}a$. In this way, a second-order ferroelectric phase transition is obtained at a critical temperature given by

$$T_0 = T_c(cl) \ , \tag{2.9}$$

where $T_c(cl)$ is defined by Eq. (1.19) and the parallel susceptibility along the c axis becomes

$$\chi = C_f/(T - T_0) \ , \tag{2.10}$$

where C_f is the Curie constant for classical free dipoles, defined in Eq. (1.23). Note that Eq. (2.10) is valid for arbitrary values of the quantum parameter γ^*, in the limit $T >> T_0$ where the dipoles become classical, whereas the equation

$$T_c(Q) \approx T_c(cl) \tag{2.11}$$

is expected to be a good approximation only in the limit $\gamma^* << 1$, as is shown in Sec. III.

III. QUANTUM-STATISTICAL TREATMENT

The eigenvalue equation for H_L is

$$H_L \psi_n(u) = \epsilon_n \psi_n(u) \tag{3.1}$$

and its eigenfunctions $\psi_n(u)$ may be written in terms of Airy functions. On the other hand, for the limited purpose of the exact determination of T_c and of the paraelectric susceptibility, only small values of the dimensionless polarization $\langle u\rangle/\frac{1}{2}a$ will be required, i.e., for this limited purpose, the polarization term H_p in Eq. (1.6) may be taken as a small quantity to be treated by perturbation theory. The perturbation expansion[38] for the density matrix

$$\rho_L(\beta) = e^{-\beta H_L} \tag{3.2}$$

may be obtained from

$$\rho_I(\beta) = 1 - \int_0^\beta H_p(\beta_1)\, d\beta_1 + \int_0^\beta H_p(\beta_1)\, d\beta_1 \int_0^{\beta_1} H_p(\beta_2)\, d\beta_2 + \cdots \ , \tag{3.3}$$

where $\rho_L(\beta) = e^{-\beta H_0}\rho_I(\beta)$, $H_p(\beta) = e^{\beta H_0} H_p e^{-\beta H_0}$, with H_0 and H_p defined by Eqs. (1.7) and (1.8), respectively. The local partition function Z_L in Eq. (1.12) may be obtained now as a power series of the molecular field A, with the result that only terms containing even powers of H_p will contribute in the calculation of $\mathrm{Tr}\rho_L$. Working in the representation where H_0 is diagonal, it turns out that the dimensionless polarization $\langle u\rangle/\frac{1}{2}a$ is of the form

$$F(\omega, \alpha) = f_1(\alpha)\omega + f_3(\alpha)\omega^3 + \cdots \ , \tag{3.4}$$

where

$$f_1(\alpha) = [15\phi_4(\alpha) - \pi^2\phi_2(\alpha)]/12\pi^2\phi_0(\alpha) \ , \tag{3.5}$$

$$\phi_s(\alpha) = \sum_{n=1}^{\infty} e^{-\alpha n^2}/n^s \ , \tag{3.6}$$

$$\alpha = 12\gamma/\tau \ , \tag{3.7}$$

$$\tau = T/T_0 \ , \tag{3.8}$$

$$\omega = Aa/E_c \ , \tag{3.9}$$

where A still contains the information coming from the molecular field in Eq. (1.9), which gives rise to the second function, G, for self-consistency as

$$G(\omega) = 2\gamma(\omega - \omega_0) \ , \tag{3.10}$$

where

$$\omega_0 = 2p_s E/E_c \ , \tag{3.11}$$

and E is the electric field appearing in Eq. (1.2). E_c is defined in Eq. (1.14). The self-consistent polarization may be obtained now, by determining the root ω_{sc} of the equation $F(\omega) = G(\omega)$ and setting $\langle u\rangle/\frac{1}{2}a = F(\omega_{sc})$. Comparing Eqs. (3.4) and (3.10), it follows that the critical temperature may be found by solving the equation:

$$f_1(\alpha_c) = 2\gamma \ , \tag{3.12}$$

where γ is the quantum parameter in Eq. (1.19) and $\alpha_c = 12\gamma/\tau_c$. Figure 1 is a plot of the function $f_1(\alpha)$, where it may be seen that $f_1(\alpha)$ is positive and increases monotonically with α, for α positive. This function approaches asymptotically the upper limit $f_{1\max} = \lim_{\alpha\to+\infty} f_1(\alpha)$, given by $f_{1\max} = (15 - \pi^2)/12\pi^2$. This quantity determines the range of values of γ for which a second-order phase transition oc-

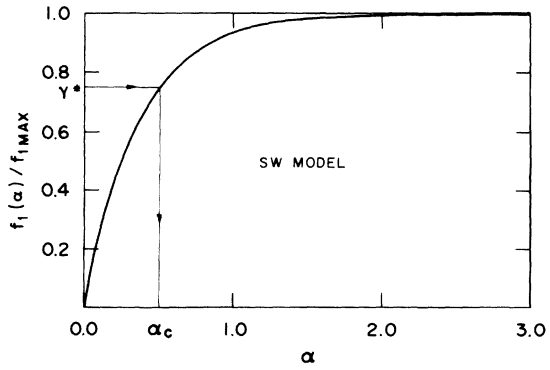

FIG. 1. Plot of the function $f_1(\alpha)$ vs α. Such a graph provides the algorithm for determination of the quantum dependence of the critical temperature, as explained in text. In the present and subsequent figures SW means the square-well local-potential model.

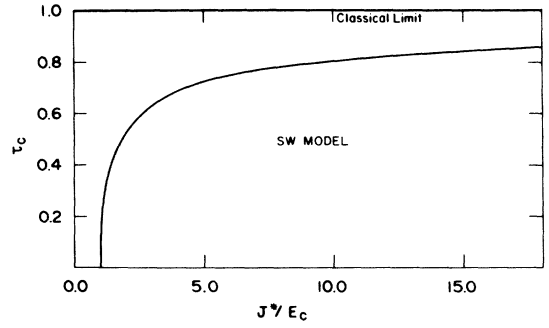

FIG. 2. Plot of the dimensionless critical temperature $\tau_c = 12\gamma_s k T_c/J^*$ vs J^*/E_c, where $J^* = \gamma_s W$, for a comparison with Fig. 5.2 of Ref. 4.

curs. In other words, only for $\gamma < \gamma_s$, where

$$\gamma_s = (15 - \pi^2)/24\pi^2 \tag{3.13}$$

is equal to 0.021 659, there exists one and only one root $\alpha_c > 0$ of Eq. (3.12) corresponding to a well-defined critical temperature. Noting that $\alpha_c = 12\gamma/\tau_c$, the solution of the equation

$$f_1(12\gamma/\tau_c) = 2\gamma \tag{3.14}$$

determines $\tau_c = T_c/T_c(cl)$ as function of $1/\gamma^*$ or γ^* which is plotted in Figs. 2 and 3, respectively. The classical limit in Eq. (1.14), corresponding to $\tau_c \to 1$ for $\gamma^* \to 0$ is well reproduced. Also note that the quantum effect, in the present model, reduces the region of existence of the ferroelectric phase, a fact that probably is model independent. In the region $\gamma \simeq \gamma_s$, the critical temperature T_c changes rapidly with γ^*, going to zero at $\gamma^* = 1$, i.e., when γ reaches what may be called the *suppressing* value γ_s, a fact that is also present in the pseudospin model.[12]

The pressure dependence of the critical temperature of ferroelectric crystals has been studied experimentally. The experimental curve for KDP obtained by Samara[39] for T_c versus pressure looks similar to that of Fig. 3. The fact that the critical temperature T_c goes to zero at a certain pressure P_s can be well accounted for by the present model if the quantum parameter γ^* is assumed to be a function of pressure which goes to one when the pressure P approaches the suppression value P_s. The results of this analysis will be published elsewhere.[40]

The parallel susceptibility χ along the c axis may also be obtained from Eqs. (3.4), (3.10), and (3.11) for arbitrary temperatures $T > T_c$,

$$\chi = \frac{2Np_s^2}{E_c} \Big/ \left(\frac{1}{f_1(\alpha)} - \frac{1}{f_1(\alpha_c)} \right) , \tag{3.15}$$

where α is defined in Eq. (3.7). Near the critical point, i.e., for $|T - T_c| \ll T_c$, the quantity

$$f_1(\alpha) \approx f_1(\alpha_c) + (\alpha - \alpha_c) f_1'(\alpha_c) ,$$

with the result that near T_c

$$\chi = C_c/(T - T_c) , \tag{3.16}$$

where

$$C_c = C_f \tau_c^2 / 6 f_1'(\alpha_c) \tag{3.17}$$

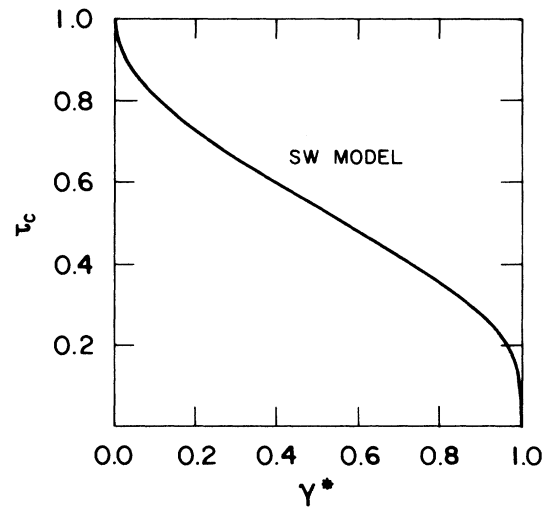

FIG. 3. Quantum (or isotope) dependence of the dimensionless critical temperature $\tau_c = T_c/T_c(cl)$. The quantum parameter γ^* in the SW model corresponds to q in the Tokunaga-Matsurbara DW model, in Fig. 6. Note the stronger quantum dependence of the SW model in the near classical region.

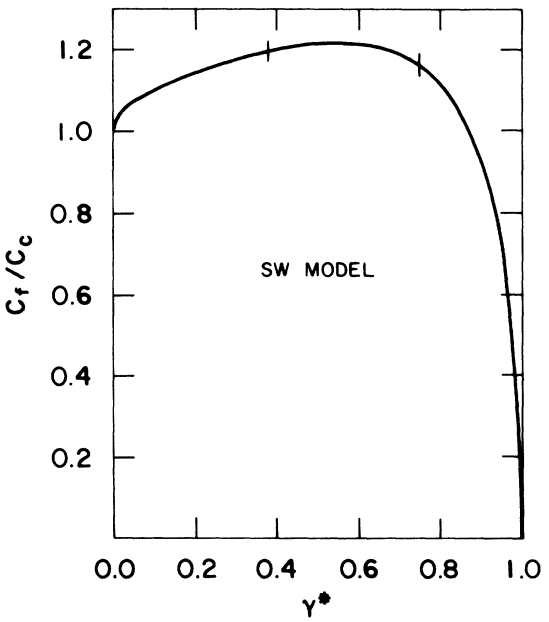

FIG. 4. Isotope dependence of the Curie constant at the critical point. Note that $C_c \to \infty$ when $T_c \to 0$ for $\gamma^* \simeq 1$, a fact that is also present in the DW model.

is the critical-point Curie constant, and C_f is defined in Eq. (1.23). Noting that τ_c and α_c are functions of γ^*, a curve for C_c/C_f vs γ^* may be constructed with the result shown in Fig. 4.

From Eq. (3.15) it is also possible to obtain the high-temperature limit for the susceptibility, with the result that Eq.(2.10) is well reproduced.

IV. SPONTANEOUS ELECTRIC POLARIZATION

The calculation of the self-consistent value of $P(T)$, the spontaneous polarization in the ferroelectric phase, for arbitrary temperatures below T_c, and for arbitrary values of $\gamma^* < 1$, is a possible but somewhat difficult task even in the MFA used above. In view of the above difficulty, in the present paper, the discussion is restricted to the γ^* dependence of the maximum polarization P_M, corresponding to the polarization value at $T=0$ K.

The self-consistent calculation of the maximum polarization P_M is a laborious task if use is made of the exact Airy functions in Eq. (3.1), even at $T=0$ K, where only the ground-state energy of H_L and its ground-state wave function are required. For this reason the use of an approximation, the variational method, becomes convenient. The trial ground-state wave function of H_L is chosen as

$$\psi_0(u) = Ce^{\delta\pi u/a}\cos(\pi u/a) \ , \tag{4.1}$$

where $\cos(\pi u/a)$ corresponds to the symmetric, unpolarized, ground-state wave function of H_0 in the paraelectric phase; δ is the variational parameter, and C is a normalization constant. The minimization of the ground-state energy

$$\epsilon_0(\delta) = \langle\psi_0|H_L|\psi_0\rangle/\langle\psi_0|\psi_0\rangle \ , \tag{4.2}$$

i.e., the equation $\partial\epsilon_0/\partial\delta=0$ may be written in the form

$$\omega = 4\pi\delta^3\Big/\left[\frac{1+3\delta^4}{(1+\delta^2)^2} - \frac{\pi^2\delta^2}{\sinh^2(\pi\delta)}\right] \ , \tag{4.3}$$

where ω is defined in Eq. (3.9), which in the zero-field case gives rise to

$$G = 2\gamma H(\delta) \ , \tag{4.4}$$

as explained in Sec. III; $H(\delta)$ stands for the right-hand side of Eq. (4.3). The second condition for self-consistency is obtained by calculating $\bar{u} = \langle\psi_0|u|\psi_0\rangle/\langle\psi_0|\psi_0\rangle$ as a function of δ, i.e, by means of the use of Eq. (4.1) and setting $F = \bar{u}/\frac{1}{2}a$ with the result that

$$F = \frac{1}{\pi\delta}\left[\frac{\pi\delta}{\tanh\pi\delta} - \frac{1+3\delta^2}{1+\delta^2}\right] \ . \tag{4.5}$$

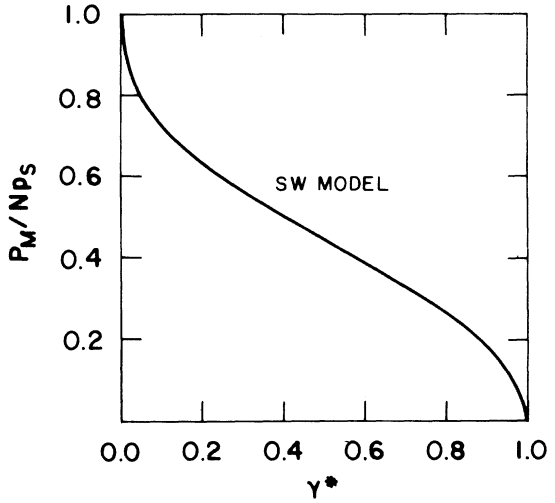

FIG. 5. γ^* dependence of the maximum spontaneous polarization P_M at absolute zero temperature.

The self-consistent value δ_{sc} of interest is the nonzero root of equation $F-G=0$. If a plot of G and F as functions of δ is made, it may be seen that a nonzero root δ_{sc} exists only for $\gamma < \gamma_{max}$, where

$$\gamma_{max} = (\pi^2-6)^2/72\pi^2 \tag{4.6}$$

is equal to 0.021 07, a value not too far from the exact suppressing value γ_S, as obtained in Eq. (3.13). The proximity of the numerical values for γ_{max} and γ_S may be considered to provide an evaluation of the precision of the variational method. For $\gamma > \gamma_{max}$ the only possible root is given by $\delta_{sc}=0$, corresponding to $P_M=0$, and this fact provides further insight as to why there can be no ferroelectric phase for $\gamma \geq \gamma_{max}$. Noting that $P_M = NZ^*e\bar{u}$, or $P_M = Np_sF_{sc}$, where p_s is defined in Eq. (1.16), a plot of P_M as a function of $\gamma^* = \gamma/\gamma_{max}$ has been constructed, with the result shown in Fig. 5.

V. TUNNELING PSEUDOSPIN MODEL

The tunneling model Hamiltonian in Eq. (1.17), modified to include a term $-\mu E\sum_j Z_j$ for the interaction between the electric dipoles and an electric field E along the c axis of the crystal, was treated by Tokunaga and Matsubara[12] (TM) in the framework of the MFA. This consists in replacing the expression $Z_j = \langle Z_j\rangle + x_j$ in Eq. (1.17), keeping all terms linear in the polarization fluctuations x_j and dropping bilinear x_ix_j products. In this way they obtained a second-order ferroelectric phase transition with a critical temperature T_c given by

$$4\Omega/F = \tanh(\Omega/kT_c) \ , \tag{5.1}$$

where Ω is the tunneling frequency and $F = \sum_j F_{0j}$.

The classical limit for T_c corresponding to $\Omega << \frac{1}{4}F$ may be obtained from Eq. (5.1) as

$$kT_c(cl) = kT_0 \equiv \tfrac{1}{4}F \ . \tag{5.2}$$

Defining the dimensionless parameters $\tau_c = T_c/T_0$ and $q = 4\Omega/F$, Eq. (5.1) may be written in the form

$$\tau_c = q/\text{arctanh}q \ . \tag{5.3}$$

The spontaneous polarization P attained at $T = 0$ was shown to be

$$P_M = N\mu(1-q^2)^{1/2} \ , \tag{5.4}$$

and the parallel electric susceptibility above T_c to be

$$\chi = N\mu^2/\Omega[\text{cotanh}(\Omega/kT) - \text{cotanh}(\Omega/kT_c)] \ , \tag{5.5}$$

which, in the limit $|T - T_c| << T_c$ may be shown to take the form

$$\chi = C_c/(T - T_c) \ , \tag{5.6}$$

with

$$C_c/C_f = \sinh^2(q/\tau_c)/(q/\tau_c)^2 \ , \tag{5.7}$$

where τ_c is determined as a function of the quantum parameter q from Eq. (5.3); C_f is Curie constant for classical dipoles given by

$$C_f = N\mu^2/k \ . \tag{5.8}$$

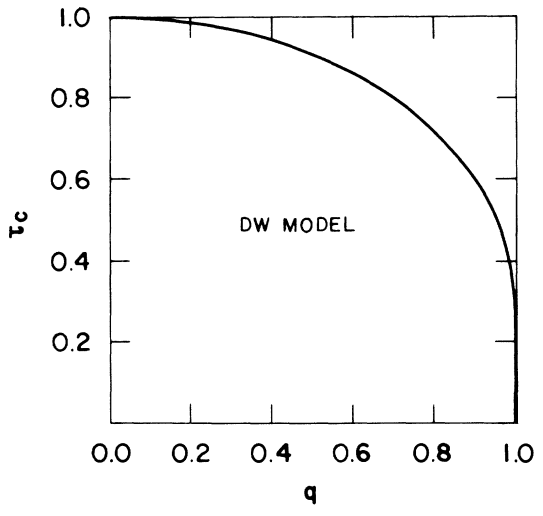

FIG. 6. Quantum dependence of the dimensionless critical temperature $\tau_c = T_c/T_c(cl)$. Note that the quantum parameter $q = 4\Omega/F$ goes to zero in the classical limit $\hbar \to 0$. In the present and subsequent figures DW means the double-well tunneling model.

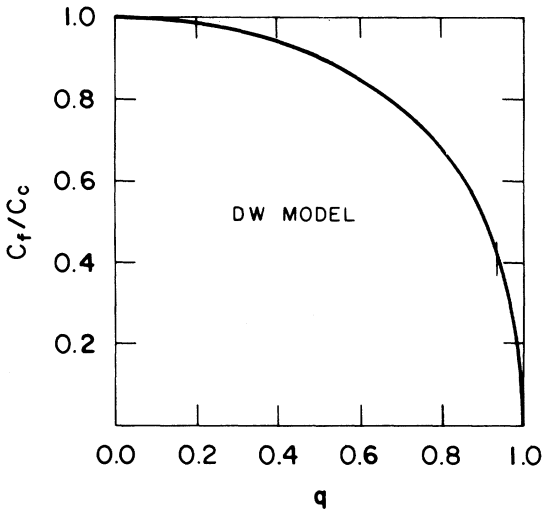

FIG. 7. Quantum dependence of the critical Curie constant.

In the high-temperature limit it may be shown that the parallel susceptibility may be written as

$$\chi = C_f/(T - T_0) \ , \tag{5.9}$$

where T_0 is defined in Eq. (5.2).

In this way the corresponding graphs for the quantum q dependence of τ_c, C_c/C_f, and $P_M/N\mu$ may be constructed with the results displayed in Figs. 6–8, which should be compared with the corresponding ones in Figs. 3–5.

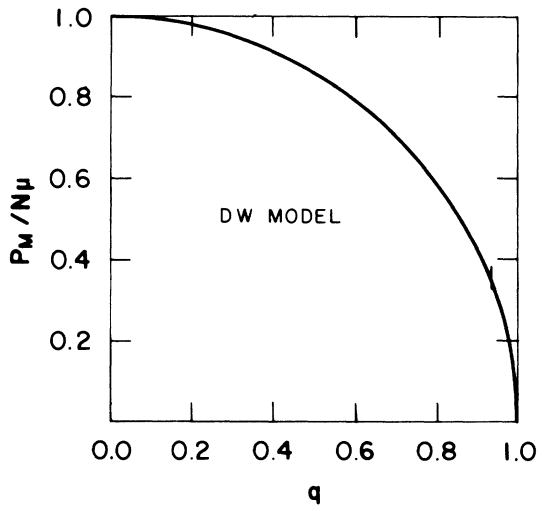

FIG. 8. Quantum dependence of the maximum spontaneous polarization P_M in the tunneling model. Comparing with Fig. 5 it may be observed the different behavior in the classical and intermediary regions.

VI. APPLICATION TO THE KH_2PO_4, KD_2PO_4 PAIR

If a comparison is made of the results obtained above for the square-well local potential in Figs. 3–5 with the corresponding ones for the central-barrier tunneling model in Figs. 6–8 the overall similarity of the results for both models becomes evident. This is even more so in the high-quantum limit corresponding to $\gamma^* \lesssim 1$ or $q \lesssim 1$ where T_c, C_c, and P_M become rapidly varying functions of the quantum parameter. Minor, nonessential, qualitative differences will occur near the classical and intermediary regions.

This new fact plus the uncertainties in the experimental data make it impossible, at the present stage, to choose between the two models, as is shown below.

Dimensionless ratios. In Table I the experimental data[41] for the critical temperature, Curie constant per unit volume near the critical point, and the maximum spontaneous polarization per unit volume are listed. Using the algorithm that leads to Fig. 3 for τ_c vs γ^* and assuming that $\gamma^*(\mathrm{H})/\gamma^*(\mathrm{D}) = 2$ as one obtains from $m(\mathrm{D})/m(\mathrm{H}) = 2$, $a(\mathrm{H}) = a(\mathrm{D})$ and $J(\mathrm{H}) = J(\mathrm{D})$, the ratio

$$\tau_c(\mathrm{D})/\tau_c(\mathrm{H}) = T_c(\mathrm{D})/T_c(\mathrm{H}) = 1.82 \quad (6.1)$$

permits the calculation of the appropriate values of γ^* with the result

$$\gamma^*(\mathrm{H}) = 0.86 \ , \quad (6.2)$$

$$\gamma^*(\mathrm{D}) = 0.43 \ . \quad (6.3)$$

The use of these values in Fig. 4, determines that

$$C_c(\mathrm{H})/C_f = 0.97 \ , \quad (6.4)$$

$$C_c(\mathrm{D})/C_f = 0.83 \ , \quad (6.5)$$

with the conclusion that the ratio

$$C_c(\mathrm{D})/C_c(\mathrm{H}) = 0.86 \ , \quad (6.6)$$

if, in Eq. (1.23), C_f is assumed to be the same for H and D. Analogously, using Eqs. (6.2) and (6.3), from Fig. 5 one obtains

$$P_M(\mathrm{H})/Np_s = 0.22 \ , \quad (6.7)$$

$$P_M(\mathrm{D})/Np_s = 0.48 \ , \quad (6.8)$$

$$P_M(\mathrm{H})/P_M(\mathrm{D}) = 0.46 \ , \quad (6.9)$$

where p_s, from Eq. (1.16), has been assumed to be isotope independent.

Proceeding analogously for the tunneling model, assuming that $F(\mathrm{H}) = F(\mathrm{D})$, we note that now there are two independent quantum parameters, q_{H} and

$$q_{\mathrm{D}} = pq_{\mathrm{H}} \ . \quad (6.10)$$

Using the results of Sec. V, and the corresponding condition Eq. (6.1), one obtains a curve (see Fig. 9) for the values of $q_{\mathrm{H}}(p)$ vs p, which are required to reproduce the observed ratio for the critical temperatures.

TABLE I. KH_2PO_4-KD_2PO_4.[a]

	H	D	Ratios
T_c (°K)	122.5 ± 0.2	223.0 ± 0.2	$T_c^{\mathrm{D}}/T_c^{\mathrm{H}} = 1.820 \pm 0.005$
$\bar{C}_c$ (°K)[b]	233 ± 4	326 ± 4	$\bar{C}_c^{\mathrm{D}}/\bar{C}_c^{\mathrm{H}} = 1.40 \pm 0.04$
$\bar{P}_M$ (μC/cm^2)	5.10 ± 0.07	6.21 ± 0.07	$\bar{P}_M^{\mathrm{D}}/\bar{P}_M^{\mathrm{H}} = 1.22 \pm 0.03$

[a]Data taken from G. Samara, Ferroelectrics 5, 25 (1973).
[b]In the present paper, barred quantities refer to unit volume.

In Eq. (5.7), τ_c is a function of q. If in that equation the quantum parameter q is replaced by $q_{\mathrm{H}}(p)$ from Fig. 9, a curve for $C_f/C_c(\mathrm{H})$ vs p is obtained in Fig. 10.

In a similar way, a curve for the possible values of $C_f/C_c(\mathrm{D})$ vs p in Fig. 11 may be obtained, if in Eq. (5.7) q is replaced by $q = q_{\mathrm{D}} = pq_{\mathrm{H}}(p)$.

From Figs. 10 and 11 one obtains Fig. 12 for the values of $C_c(\mathrm{D})/C_c(\mathrm{H})$, consistent with the ratio for the critical temperatures, determined as a function of $p = \Omega(\mathrm{D})/\Omega(\mathrm{H})$.

Along the same lines, using Eq. (5.4), the values of $P_M(\mathrm{H})$, $P_M(\mathrm{D})$, and $P_M(\mathrm{H})/P_M(\mathrm{D})$ consistent with the observed ratio for the critical temperatures are displayed in Figs. 13–15, respectively.

As one can see in Figs. 12 and 15, the largest attainable value of $C_c(\mathrm{D})/C_c(\mathrm{H})$ is 0.41, whereas for $P_M(\mathrm{H})/P_M(\mathrm{D})$ the maximum value corresponds to 0.35 both occurring at $p = 0$.

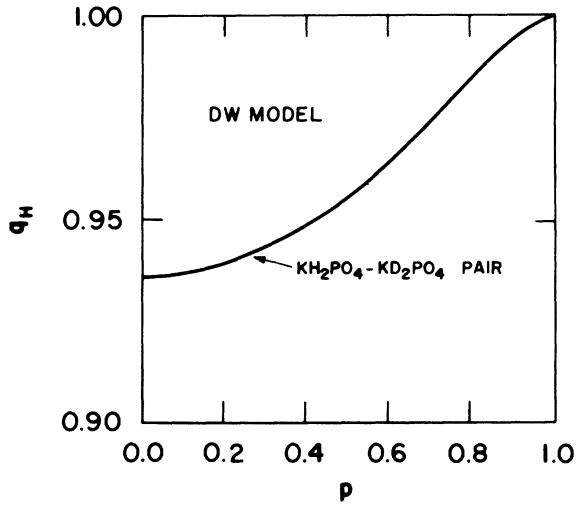

FIG. 9. Possible values of the quantum parameter q_{H} required to reproduce the experimental ratio $T_c(\mathrm{D})/T_c(\mathrm{H})$ for the KDP pair.

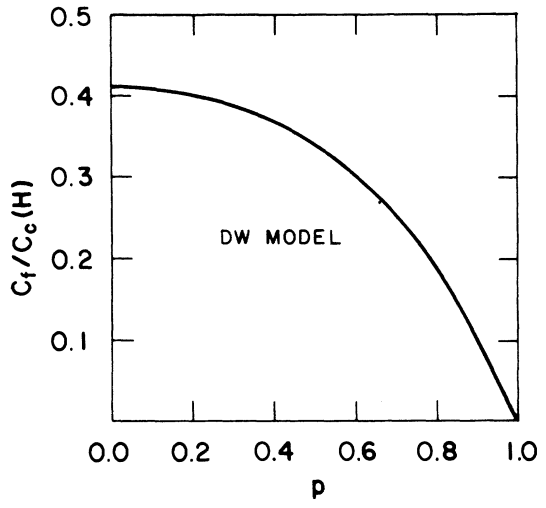

FIG. 10. Possible values of the critical Curie constant in KH_2PO_4 consistent with the experimental value of $T_c(D)/T_c(H)$.

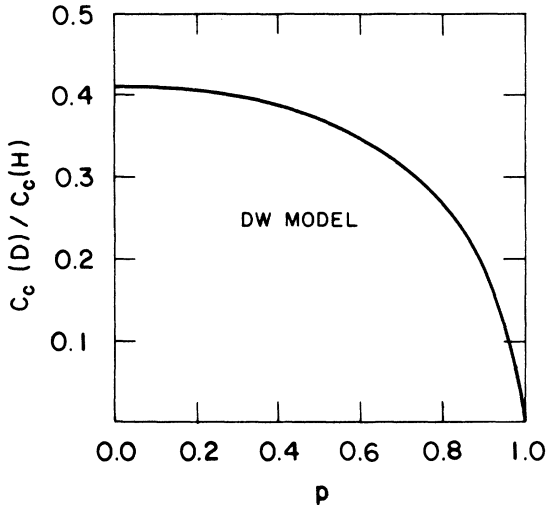

FIG. 12. Possible values of $C_c(D)/C_c(H)$ consistent with the experimental value of $T_c(D)/T_c(H)$ for the KDP pair.

The situation is summarized in Table II, where the SW model means the square-well model whose corresponding numerical values come from Eqs. (6.6) and (6.9), whereas the DW model means the double-well tunneling model.[12] In Table II it becomes evident first of all that the DW model is certainly not better than the simple SW potential even having at its disposition one more adjustable parameter (p). Both models fail quantitatively. If the corresponding extra parameter $p=\gamma^*(D)/\gamma^*(H)$ is introduced in the SW model, i.e., if $V_s(u)$ for D is assumed different from that for H, it is quite probable that better values for the ratios for C_c and P_M would be obtained.

Magnitudes of physical quantities. As discussed in Secs. III–V the critical temperature, Curie constant at the critical point, and the maximum value attained by the spontaneous polarization are scaled in terms of the quantities T_0, $\bar{C}_f$, and $\bar{N}p_s$, respectively, for the SW model; for the DW model p_s must be replaced by μ. Since $p=0$, was found to be the best choice for the double-well model, corresponding to $q_D=0$, it becomes convenient to use $T_c(D)$, $\bar{C}_c(D)$ instead of the corresponding quantities for KH_2PO_4, in both SW and DW models. This leads to the construction of Table III, where the line of values for the DW model

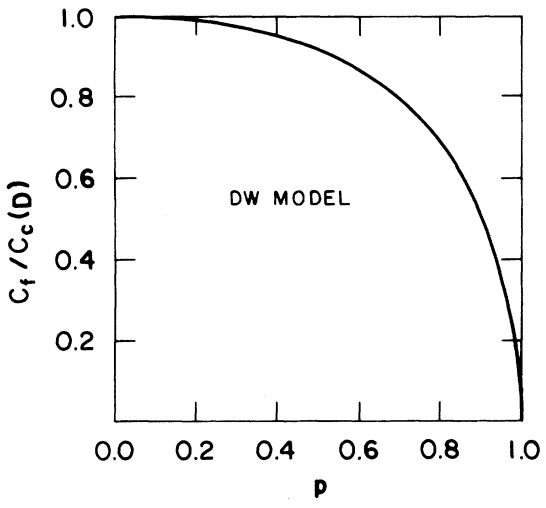

FIG. 11. Same as in Fig. 10 for KD_2PO_4.

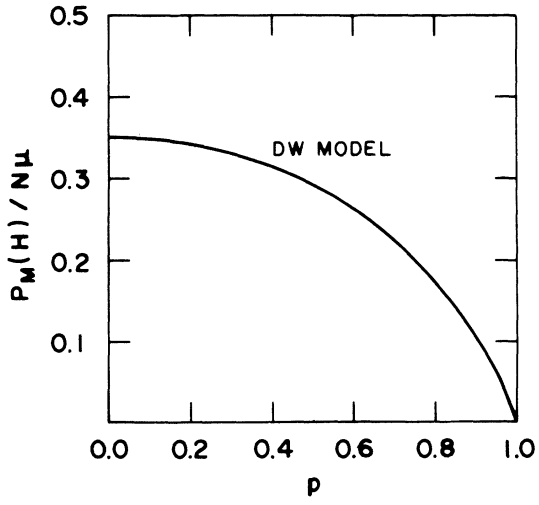

FIG. 13. Allowed values of the maximum polarization P_M of KH_2PO_4 consistent with the experimental value of $T_c(D)/T_c(H)$.

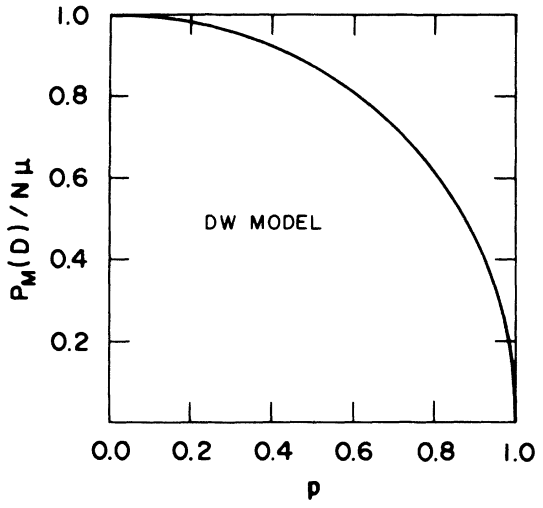

FIG. 14. Same as in Fig. 13, now for KD_2PO_4.

corresponds to the classical limit ($q_D=0$) whereas for the SW model, the value of $\tau_c(D)$ may be obtained in Fig. 3 for $\gamma^*(D)=0.43$, and the remaining dimensionless quantities come from Eqs. (6.5) and (6.8), respectively. Using now only the experimental values of $T_c(D)$ and $\bar{C}_c(D)$ and the values listed in the second and third column of Table III, one obtains $T_0(SW)=387\,^\circ K$ and $\bar{C}_f(SW)=395\,^\circ K$ as well as $T_0(DW)=223\,^\circ K$ and $\bar{C}_f(DW)=326\,^\circ K$, which are listed in Table IV.

Assuming a dipolar nature for the hydrogen-hydrogen interaction in both models, and recalling that the classical limit for both cases corresponds to a dominant dipole-dipole character, where the critical

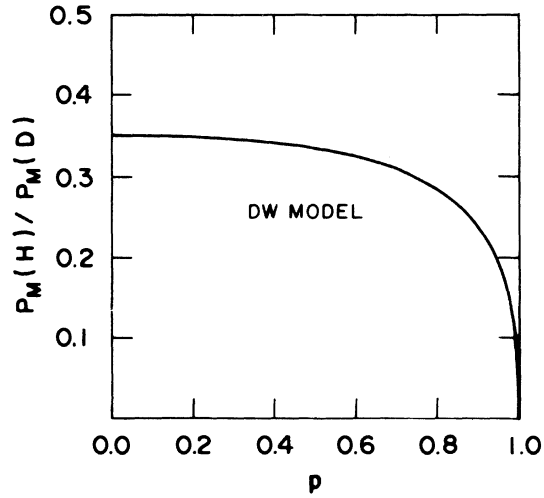

FIG. 15. Allowed values of the ratio of maximum polarizations $P_M(H)/P_M(D)$ consistent with the experimental value of $T_c(D)/T_c(H)$ for the KDP associated pair.

TABLE II. Predicted ratios for C_c and P_M consistent with the experimental value for $T_c(D)/T_c(H)$ in the various models discussed in text compared with the corresponding experimental ratios in Table I.

	$C_c(D)/C_c(H)$	$P_M(H)/P_M(D)$
Expt.[a]	1.40	0.82
SW model	0.86	0.46
DW model	≤ 0.41	≤ 0.35
Novakovic[b]	...	0.43

[a]From Table I.
[b]Reference 7.

temperature would become equal to $T_0=W/12k$ or $T_0=F/4k$ in SW and DW cases, respectively, the quantity kT_0 defines the basic energy scale for the problem in both models.

In the square-well model, noting that

$$W=8\sum_{j\neq 0} p_s^2(3\cos^2\theta_j-1)/r_j^3 \ , \tag{6.11}$$

where θ_j is the polar angle for $\vec{r}_j$ with respect to the c axis of the crystal, where $\vec{r}_j$ is the equilibrium position of the centroid of molecule j, one obtains

$$kT_0(SW)=f\bar{N}p_s^2 \ , \tag{6.12}$$

where $\bar{N}$ is the number of KDP molecules per unit volume, and f is a dimensionless structure-dependent parameter (see Appendix). Recalling that

$$\bar{C}_f(SW)=\bar{N}p_s^2/3k \ , \tag{6.13}$$

using the experimental x-ray value[6] for $\bar{N}=4/V_c$, where V_c is the unit-cell volume, as well as the numerical values obtained above for T_0 and $\bar{C}_f$, Eqs. (6.12) and (6.13) can be solved for the determination of the two unknowns f and p_s, whose values are listed in Table IV.

For the double-well tunneling model, recalling the notation correspondence between the papers of TM[12] and Blinc[10] in which $kT_0=\frac{1}{4}F=\frac{1}{4}J(TM)$

$$kT_0(DW)=f\bar{N}\mu^2 \tag{6.14}$$

as one can identify in the latter reference, noting that τ_c in the present paper, Eq. (5.3), corresponds to $\tau_c=2Z(\alpha)$ in that paper. The corresponding equa-

TABLE III. Predicted values of dimensionless quantities for KD_2PO_4, consistent with the experimental value of $T_c(D)/T_c(H)$, in both models; see text.

	$T_c(D)/T_0$	$\bar{C}_c(D)/\bar{C}_f$	$\bar{P}_M(D)/\bar{N}$
SW	0.58	0.83	$0.48p_s$
DW	1.00	1.00	1.00μ

TABLE IV. Calculated values of T_0 and $\bar{C}_f$ obtained from Table III using the experimental values of $T_c(\mathrm{D})$ and $\bar{C}_c(\mathrm{D})$ in Table I. Knowledge of the values of T_0 and $\bar{C}_f$ allows for a determination of the quantities f and p_s in both models.

	T_0 (°K)	$\bar{C}_f$ (°K)	(c Å)	f	$\bar{P}_M(\mathrm{D})_{\mathrm{calc}}$ (μC/cm^2)
SW	387	395	$p_s=0.82$	0.33	6.6
DW	223	326	$\mu=0.43$	0.68	7.2

tion for $\bar{C}_f$ is

$$\bar{C}_f(\mathrm{DW})=\bar{N}\mu^2/k \tag{6.15}$$

Using Eqs. (6.14) and (6.15), as well as the above determined values for $T_0(\mathrm{DW})$ and $\bar{C}_f(\mathrm{DW})$, the corresponding values for f and μ have been determined and listed in Table IV, where it should be noted that μ is not necessarily the same as p_s for the SW model, whereas f should have the same value in both models.

The values listed in the fourth column of Table III have not been used yet. Using now the values obtained above for p_s and μ as well as the x-ray value of $\bar{N}$, the numerical values for $\bar{P}_M(\mathrm{D})/\bar{N}p_s$ listed in Table III allow a calculation of $\bar{P}_M(\mathrm{D})$ for both SW and DW models, which are displayed in the last column of Table IV, and which may be compared with the known experimental value[41] of $\bar{P}_M(\mathrm{D})=6.2$ μC/cm^2. Comparing the values of $\bar{P}_M(\mathrm{D})$ so obtained one can see that quite reasonable values have now been obtained, but here again the square-well model gives better agreement with experiment.

As for the calculated values of T_0 and $\bar{C}_f$ listed in Table IV no experimental data are available from high-temperature (classical) behavior of the parallel electric susceptibility, probably because of the low melting-point of these materials.

As a curiosity, if we recall Eqs. (1.21) and (2.9), which define γ^* and T_0, respectively, one obtains

$$E_c(\mathrm{H})=12\gamma_s\gamma^*(\mathrm{H})kT_0 \ ,$$

where $\gamma^*(\mathrm{H})=0.86$ from Eq. (6.2) and $T_0=387$ °K from Table IV, $\gamma_s=0.0216$ from Eq. (3.13), with the result

$$E_c(\mathrm{H})=7.4 \text{ meV} \ , \tag{6.16}$$

which differs from the value 6.8 meV given by Pirenne[9] only because a more recent value for $T_c(\mathrm{D})$ has been used in the present analysis. From the definition of E_c in Eq. (1.14) one obtains for the width of the square-well potential the value

$$a=1.66 \text{ Å} \ , \tag{6.17}$$

which may be compared with the available space existing between the two oxygen ions in KH_2PO_4, i.e., $D(OO)-2r_0\approx(2.50-1.32)$ Å $=1.18$ Å as one obtains from BP[6] and the covalent radius for oxygen in a monography by Speakman.[15] Noting that $p_s=\frac{1}{2}Z^*ea$ from Eq. (1.16), the numerical value of Z^* may be estimated by using Eq. (6.17) and the value of p_s listed in Table IV with the result

$$Z^*=0.99 \ .$$

The results above obtained seem to indicate that the bottom of the local effective potential may be quite flat.

The failure of the DW tunneling model to describe quantitatively the observed values for $C_c(\mathrm{H})/C_c(\mathrm{D})$ and $P_M(\mathrm{H})/P_M(\mathrm{D})$ (see Table II) led Tokunaga and Matsubara to consider such a contradiction with experiment as due to the use of the molecular-field approximation. Taking into account the short-range correlations among the four nearest-neighbor hydrogen atoms to a PO_4 group, in similar manner to the model of Slater[30] and Takagi[42] and neglecting all the other-than-nearest dipole-dipole interactions, TM[12] obtained a sharp second-order ferroelectric phase transition, with a choice of $n=5$. In this way they obtained a curve (see their Fig. 6) for the isotope dependence of $T_c=T_c(q)$, where $q=\Omega_T/\epsilon_0$ is the new quantum parameter. Such a curve looks quite similar to that of Fig. 3 obtained in the present SW model for $\tau_c(\gamma^*)$. The predicted values for $C_c(\mathrm{H})/C_c(\mathrm{D})$ and $P_M(\mathrm{H})/P_M(\mathrm{D})$ in the above cluster approximation were not given by TM in that paper. They only state that the cluster approximation is inadequate to describe the relative lack of sensitivity of C_c and P_M to deuteration.

KH_2PO_4-KD_2PO_4 mixtures. The concentration dependence of the static ferroelectric properties of KDP-DKDP solid solutions has attracted the attention of a number of investigators.[41] Proceeding in a form similar to that of TM, an effective quantum parameter γ^* is assumed for each solid solution, with a deuterium-concentration dependence given by

$$\gamma^*(x)=(1-x)\gamma_{\mathrm{H}}^*+x\gamma_{\mathrm{D}}^* \tag{6.18}$$

for the SW model and,

$$q(x)=(1-x)q_{\mathrm{H}}+xq_{\mathrm{D}} \tag{6.19}$$

for the DW model, where x is the deuterium concentration, $\gamma_{\mathrm{H}}^*=0.86$ and $\gamma_{\mathrm{D}}^*=0.43$ are taken from Eqs. (6.2) and (6.3), and $q_{\mathrm{H}}=0.94$ as shown in Fig. 9 for the best choice $p=0$ and $q_{\mathrm{D}}=0$ for KDP pair. In order to make use of the experimentally determined[41] values for $T_c(x)$, $C_c(x)$, and $\bar{P}_M(x)$, if in Figs. 3–5 one replaces γ^* by the values $\gamma^*(x)$ of Eq. (6.18), tables could be constructed for $T_c(x)/T_0$, $\bar{C}_c(x)/\bar{C}_f$, and $\bar{P}_M(x)/\bar{N}p_s$ for x in the range $0\leq x\leq 1$. Assuming, as we have done above, that T_0, $\bar{C}_f$, and $\bar{N}p_s$ are isotope independent, curves for $T_c(x)/T_c(1)$, $\bar{C}_c(x)/\bar{C}_c(1)$, and $\bar{P}_M(x)/P_M(1)$ as functions of x may be obtained with the result displayed in Figs. 16–18 in full lines.

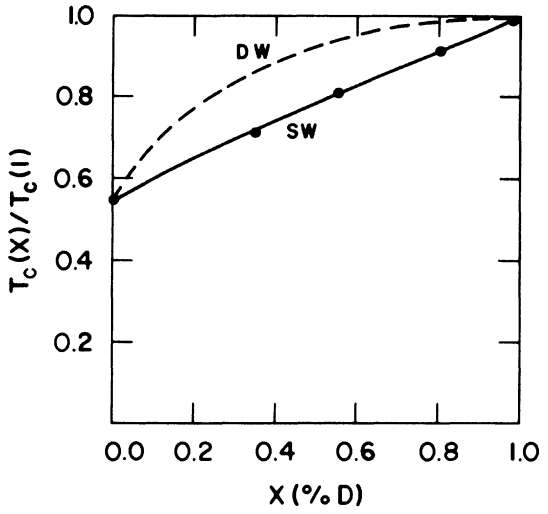

FIG. 16. Deuterium-concentration dependence of the critical temperature in solid KH_2PO_4-KD_2PO_4 solutions, for the square-well and the tunneling double-well model.

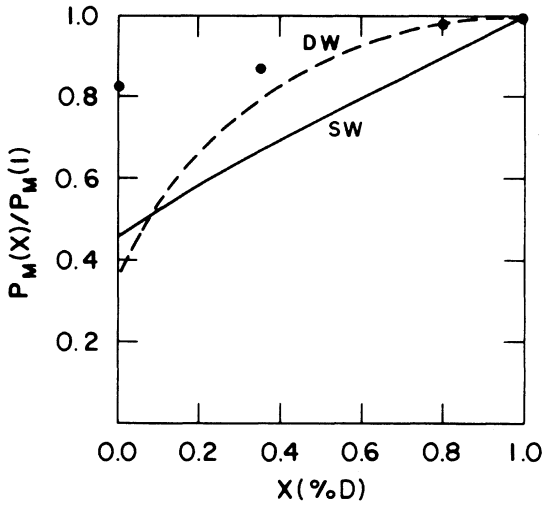

FIG. 18. Deuterium-concentration dependence of the maximum polarization in solid KH_2PO_4-KD_2PO_4 solutions, for the SW and the DW model.

Using the same method for the DW model, from Figs. 6–8, the corresponding curves for the concentration dependence are shown, for a comparison, also in Figs. 16–18 in dashed lines. Due to the difficulties involved in the precise determination of deuterium concentration in each specimen, the experimental points in Figs. 16–18 are scarce. On the other hand Fig. 16 may be used to provide a scale for the determination of the deuterium concentration, $x = x(T_c)$ if the values of T_c are known. In this way, replacing in Figs. 17 and 18 the values so obtained for $x = x(T_c)$, the graphs of Figs. 19 and 20 may be obtained for the SW and DW models. Now, many more experimental points may be used from the reported data,[41] even for those cases where the deuterium contents were not known.

As can be seen in Fig. 16 the MFA, as applied to the SW model, describes quantitatively the concentration dependence of T_c, whereas the DW model is not

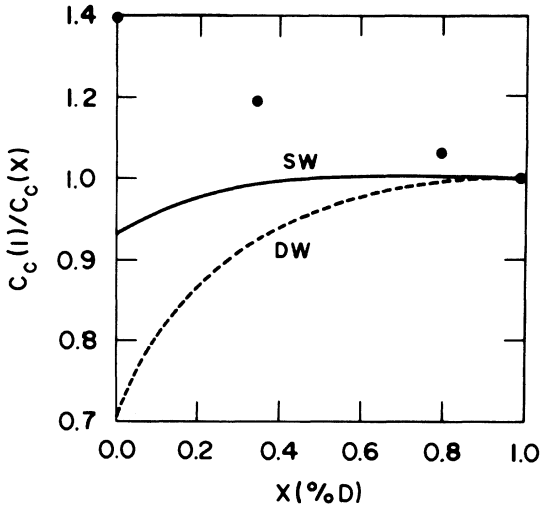

FIG. 17. Deuterium-concentration dependence of the critical Curie constant in solid KH_2PO_4-KD_2PO_4 solutions, for both models.

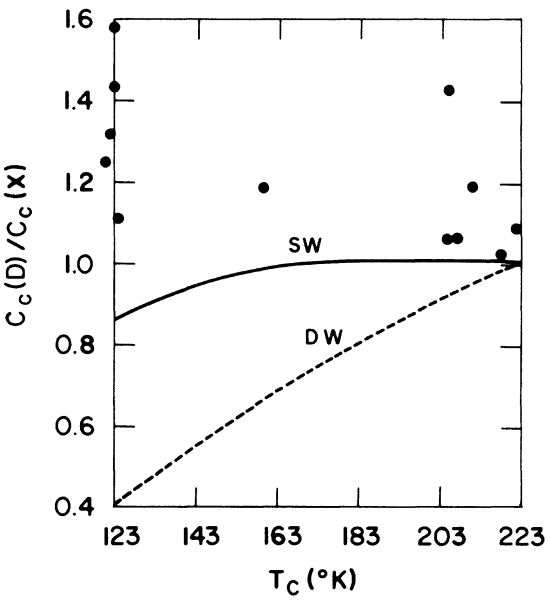

FIG. 19. Correlation between the Curie constants C_c and the critical temperatures in solid KH_2PO_4-KD_2PO_4 solutions for both models. $C_c(D)$, the constant appropriate for pure KD_2PO_4, has been used as a normalization constant. The experimental points were taken from Samara (Ref. 41) and references therein.

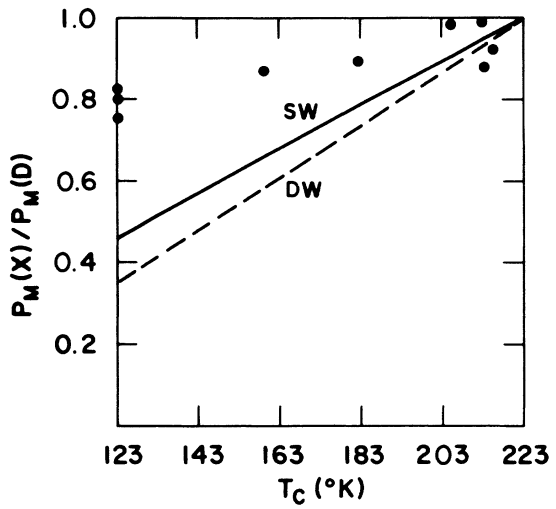

FIG. 20. Same as Fig. 19, now for P_M.

consistent with the experimental data. The near linearity predicted by the SW model for the x dependence of T_c is related to the linearity of Fig. 3, in the region between γ_D^* and γ_H^*. The inconsistency of the DW prediction with the experimental data in Fig. 16, led TM to attribute the difficulty to the use of the MFA. But from Fig. 16, we can conclude that this is not necessarily so. In any event, with the use of the cluster approximation, they succeeded in obtaining consistency between the DW model and experimental data for $T_c(x)$ (see their Fig. 7).

In Figs. 17 and 18, once again we can see that both models fail quantitatively, but still the square-well model is closer to the overall experimental data. Noting that the SW prediction in Fig. 18 came from the use of the variational method, as described in Sec. IV, it is possible that the exact calculation by means of the appropriate Airy functions may lead to an improvement. In Fig. 19 one can see that in spite of the dispersion of the experimental points, they are all closer to the SW prediction as compared to that for the double-well tunneling model.

VII. DISCUSSION AND CONCLUSIONS

The oversimplified square-well model considered here seems to be inadequate to describe infrared and Raman frequencies associated with the hydrogen motion in these quantum ferroelectrics. On the other hand, we cannot exclude the possibility that a no-barrier modification of the above square-well model, or a nearly harmonic one-minimum local potential[43] may become adequate to describe not only the phase transition, the strong or moderate isotope dependence, but the infrared- and Raman-observed H-motion frequencies as well.

According to Wiener *et al.*[44] the broad ir bands observed in KDP at 2400 and 2750 cm^{-1} have been discussed extensively in the literature but their origin is not yet clear; the corresponding KD_2PO_4 bands are shifted to 1730 and 2000 cm^{-1}; all these peaks seem to be unconnected with the ferroelectric phase transition since the transition was shown not to affect them; the frequency ratios $\nu(H)/\nu(D)$ are, respectively, 1.39 and 1.37, i.e., very close to the $\sqrt{2}$ harmonic ratio, and this fact may be considered to favor the displacive one-minimum near-harmonic model for KDP. Inclusion of corrections to above ratios, coming from vibrations transversal to the bond as discussed by Pirenne[43] may even bring those ratios closer to 1.41. In other words, the use of those infrared bands does not seem adequate to discriminate between the displacive (one-minimum) or the order-disorder (double-well) character of those ferroelectric crystals, at least until much more accurate calculations and experiments become available.

In the model suggested by Novakovic[7] for KDP the local potential $V_s(u)$ is replaced by a full many-body problem, but still use is made of a representation envolving four linearly independent local wave functions in a manner that looks similar to Slater-Takagi-Blinc model. Taking into account the short-range nearest-neighbor interactions among the four hydrogen bonds close to a KDP molecule, he succeeded in obtaining consistency with the laser-excited Raman lines observed by Kaminow *et al.*[45] at room temperature in single crystals of pure and deuterated samples of KDP. No experiments on the temperature or transition dependence of the 2705, 2360, and 1790 cm^{-1} Raman bands for KDP, as well as for those at 1990, 1770, and 1370 cm^{-1} for DKDP seem to be available. The near-harmonic ratios for the corresponding H and D Raman frequencies may be considered again[43] as an argument in favor of the simple near-harmonic one-minimum local-potential character for KDP, or being more precise, the above Raman frequencies may be considered not to provide a clear discrimination between Novakovic model and the one-minimum local-potential model. Besides that the above many-body model, with the neglect of the long-range component of the dipole-dipole interaction, seems to allow only for a second-order phase transition as opposed to experimental evidence already mentioned for a first-order phase transition.

As a result of the above discussion, it may be stated that the isotope dependence of T_c, C_c, and P_M as well as the H motion above assigned infrared and Raman frequencies do not provide yet a clear discrimination between the displacive and the order-disorder character for KDP.

ACKNOWLEDGMENTS

This research was supported by FAPESP and CNPq.

APPENDIX

As a curiosity let us consider the possible dipole-dipole origin for the hydrogen-hydrogen J_{ij} coupling in Eq. (1.2). The direct dipole-dipole interaction between the KP dipole of molecule i and that of molecule j is given by

$$+\frac{1}{r_{ij}^3}(\vec{P}_i\cdot\vec{P}_j-3\vec{P}_i\cdot\hat{r}_{ij}\hat{r}_{ij}\cdot\vec{P}_j) \quad , \tag{A1}$$

where $\vec{P}_i$ is the electric dipole of the KP ion pair in molecule i, r_{ij} is the distance between $(KP)_i$ and $(KP)_j$, and $\hat{r}_{ij}$ is the unit vector along the line connecting i and j. Now assume that the displacements of the K and P ions occur essentially along the c axis of the crystal, i.e., that

$$\vec{P}_j \cong P_{jz}\hat{Z} \quad , \tag{A2}$$

where P_{zj} is not the absolute value of the dipole but its component along the c axis, which may change sign according to Eq. (1.1). Equation (A2) corresponds to assume that both K and P ions have a cigar-shaped Debye-Waller factor directed along the c axis, corresponding to relatively small displacements transversal to c axis. Using now the strong H-KP coupling by means of Eq. (1.1), and replacing Eq. (A2) in Eq. (A1), the interaction energy between site 0 and site j becomes

$$-\frac{p_s^2}{(\frac{1}{2}a)^2}\frac{1}{r_{0j}^3}(3\cos^2\theta_j-1)u_0u_j \quad , \tag{A3}$$

where use has been made of the definition for p_s in Eq. (1.16); in Eq. (A3), θ_j is the polar angle of vector $\hat{r}_{0j}$. Consequently the molecular-field energy W, in Eq. (1.15) becomes

$$W=8p_s^2\sum_{j\neq 0}\frac{1}{r_{0j}^3}(3\cos^2\theta_j-1) \tag{A4}$$

and the structure-dependent parameter f defined in Eq. (6.12) becomes

$$f=\tfrac{1}{6}\sum_{j\neq 0}\frac{1}{(r_{0j}/D)^3}(3\cos^2\theta_j-1) \quad , \tag{A5}$$

where $D^3=V_c$ is the unit-cell volume. The best method for an evaluation of Eq. (A5) is the Ewald method. The angle θ for which $3\cos^2\theta-1=0$ corresponds to $\theta_c\cong 55°$. The fact that the factor f may be positive in KDP-type ferroelectrics may be explained if it is observed that, other considerations being equal, the angular average of $3\cos^2\theta-1$ is zero, since $\langle\cos^2\theta\rangle=\frac{1}{3}$. For a tetragonal or orthorrombic "squashed" structures the nearest neighbors to a central site correspond to $\cos\theta=\pm 1$, where $3\cos^2\theta-1$ attains its maximum value $+2$.

---

*Work submitted in partial fulfillment of the requirements for the Ph.D degree.

[1]W. Känzig, *Ferroelectrics* and *Antiferroelectrics* (Academic, New York, 1957).

[2]F. Jona and G. Shirane, *Ferroelectric Crystals* (Pergamon, New York, 1962).

[3]E. Fatuzzo and W. J. Merz, *Ferroelectricity* (North-Holland, Amsterdam, 1967).

[4]R. Blinc and B. Zeks, *Soft Modes in Ferroelectrics and Antiferroelectrics* (North-Holland, Amsterdam, 1974).

[5]M. E. Lines and A. M. Glass, *Principles and Applications of Ferroelectrics and Related Materials* (Clarendon, Oxford, 1977).

[6]G. E. Bacon and R. S. Pease, Proc. R. Soc. London Ser. A 220, 397 (1953); 230, 359 (1955).

[7]L. Novakovic, J. Phys. Chem. Solids 31, 431 (1970).

[8]F. Unterleitner, Y. Okaya, K. Vedam, and R. Pepinsky, Abstracts Annual Meeting American Crystallographic Association, Ithaca, New York, 1959 (unpublished).

[9]J. Pirenne, Physica (Utrecht) 15, 1019 (1949).

[10]R. Blinc and D. Hadzi, Mol. Phys. 1, 391 (1958); R. Blinc, J. Phys. Chem. Solids 13, 204 (1960).

[11]P. G. de Gennes, Solid State Commun. 1, 132 (1963).

[12]M. Tokunaga and T. Matsubara, Prog. Theor. Phys. 35, 581 (1966); see also M. Tokunaga, *ibid.* 36, 857 (1966).

[13]K. K. Kobayashi, J. Phys. Soc. Jpn. 24, 497 (1968).

[14]M. E. Lines, Phys. Rev. B 9, 950 (1974).

[15]J. C. Speakman, *The Hydrogen Bond and Other Intermolecular Forces* (Chemical Society, Burlington House, London, 1975).

[16]S. N. Vinogradov and R. H. Linnell, *Hydrogen Bonding* (Van Nostrand, New York, 1971).

[17]W. C. Hamilton and J. A. Ibers, *Hydrogen Bonding in Solids* (Benjamin, New York, 1968), see Fig. 2.7.

[18]M. L. Huggins, J. Phys. Chem. 40, 723 (1937); see Figs. 1 and 2.

[19]R. Blinc, in *Proceedings of the International School of Physics* (North-Holland, Amsterdam, 1976), p. 377.

[20]C. Reid, J. Chem. Phys. 30, 182 (1959); see also W. P. Mason, Phys. Rev. 72, 854 (1947).

[21]A. R. Ubbelohde and I. Woodward, Proc. R. Soc. London Ser. A 179, 399 (1941-42); A. R. Ubbelohde, *ibid.* 173, 417 (1939).

[22]L. Onsager, Phys. Rev. 65, 117 (1944).

[23]F. J. Dyson, E. H. Lieb, and B. Simon, Phys. Rev. Lett. 37, 120 (1976); J. Stat. Phys. 18, 335 (1978).

[24]G. T. Rado and H. Suhl, *Magnetism* (Academic, New York, 1966).

[25]C. Scherer and I. Aveline, Phys. Status Solidi B 75, 465 (1976).

[26]E. H. Stanley, *Introduction to Phase Transitions and Critical Phenomena* (Clarendon, Oxford, 1971).

[27]C. Kittel, *Quantum Theory of Solids* (Wiley, New York, 1963).

[28]D. C. Mattis, *The Theory of Magnetism: An Introduction to*

the Study of Cooperative Phenomena (Harper, New York, 1965).
[29]M. A. F. Scarparo, R. S. Katiyar, R. Srivastava, and S. P. S. Porto, Phys. Status Solidi B 90, 543 (1978).
[30]J. Stater, J. Chem. Phys. 9, 16 (1941).
[31]M. De Quervain, Helv. Phys. Acta 17, 509 (1944).
[32]J. Kobayashi, Y. Uesu, and Y. Enomoto, Phys. Status Solidi B 45, 293 (1973).
[33]R. P. Craig, Phys. Lett. 20, 140 (1966); S. Tsunekawa, Y. Ishibashi, and Y. Takagi, J. Phys. Soc. Jpn. 27, 919 (1969).
[34]W. Reese, Phys. Rev. 181, 905 (1969).
[35]J. W. Benepe and W. Reese, Phys. Rev. B 3, 3032 (1971).
[36]M. Chabin and F. Gilletta, Ferroelectrics 15, 149 (1977).
[37]H. B. Silsbee, E. A. Uehling, and V. H. Schmidt, Phys. Rev. 133, A165 (1964).
[38]See for example K. Huang, *Statistical Mechanics* (Wiley, New York, 1963).
[39]G. A. Samara, Phys. Rev. Lett. 27, 103 (1971).
[40]Paulo R. P. Silva and J. A. Roversi (unpublished).
[41]G. A. Samara, Ferroelectrics 5, 25 (1973); see also references therein.
[42]U. Takagi, J. Phys. Soc. Jpn. 3, 271 (1948).
[43]J. Pirenne, Physica (Utrecht) 21, 971 (1955).
[44]E. Wiener, S. Levin, and I. Pelah, J. Chem. Phys. 52, 2881 (1970); see also A. S. Barker, Jr. and M. Tinkham, J. Chem. Phys. 38, 2257 (1963); A. N. Lazarev and A. S. Zaitseva, Sov. Phys. Solid State 2, 2688 (1961).
[45]I. P. Kaminow, R. C. C. Leite, and S. P. S. Porto, J. Phys. Chem. Solids 26, 2085 (1965).